

2002

Tube By Tube Simulation For Global Design Of R-407C Evaporators

G. Bigot
Ecole des Mines de Paris

D. Clodic
Ecole des Mines de Paris

Follow this and additional works at: <http://docs.lib.purdue.edu/iracc>

Bigot, G. and Clodic, D., "Tube By Tube Simulation For Global Design Of R-407C Evaporators" (2002). *International Refrigeration and Air Conditioning Conference*. Paper 548.
<http://docs.lib.purdue.edu/iracc/548>

This document has been made available through Purdue e-Pubs, a service of the Purdue University Libraries. Please contact epubs@purdue.edu for additional information.

Complete proceedings may be acquired in print and on CD-ROM directly from the Ray W. Herrick Laboratories at <https://engineering.purdue.edu/Herrick/Events/orderlit.html>

R5-3

TUBE BY TUBE SIMULATION FOR GLOBAL DESIGN OF R-407C EVAPORATORS

Gaëtan Bigot, Denis Clodic

Ecole des Mines de Paris, Center for Energy Studies - 60, boulevard Saint-Michel – F – 75272 Paris Cedex 06
Phone: +33 1 40 51 92 49 – Fax: +33 1 46 34 24 91 bigot@cenerg.ensmp.fr, clodic@cenerg.ensmp.fr

ABSTRACT

Air to air split systems formerly used pure refrigerants as R-22 and now many are developed with R-410A. R-407C, which shows a temperature glide during condensation and evaporation, is less used for these small capacity systems. A detailed experimental study has been performed and a tube by tube model has been developed in order to reach a better understanding of the links between internal heat exchange coefficients, pressure drops, and external air velocity. A development of multiple-row heat exchangers permits to take advantage of the temperature glide of the refrigerant blend in order to limit the temperature difference between the airflow and the heat exchange surface. The study compares R-22 and R-407C performances for different designs of evaporators showing possible actions to define optimization criterion integrating air and R-407C mass flow rates. Taking into account the evaporator optimization, it is possible to reach global higher performances for air-to-air split systems using R-407C compared to pure refrigerant performances.

1. INTRODUCTION

R-407C is a nonazeotropic refrigerant blend with a 5 to 7K temperature glide for typical evaporator operating pressures. To take advantage of this temperature glide in AC systems, a counter-cross flow shall be arranged between the refrigerant and the airflow. The study of the evaporator is complex due to a number of possible circuit arrangements. To analyze those different options, a detailed model has been developed called AIR_HEX. In this study AIR_HEX has been used to determine the performances of a three-row evaporator. A new criterion has been established to minimize the difference of temperatures between air flow and refrigerant all along the air coil. The results indicate that for a given air mass flow rate and a given evaporator design an optimum refrigerant mass flow rate exists.

2. FINNED-TUBE EVAPORATOR MODEL AIR_HEX

2.1 Description Of The Model

The modeling scheme is “tube-by-tube” and allows to design complex refrigerating circuits. The program recognizes each tube as a separate entity for which it calculates heat transfer. These calculations are based on refrigerant and air thermodynamic properties, and mass flow rates. Simulations begin with the inlet refrigerant tube and proceeds to successive tubes along the refrigerant path. For counter-current flow arrangement, the air temperature is only known for the tubes in the first row and shall be calculated for all tubes. The program requires several iterations through the refrigerant circuit, and at each step, inlet air parameters are updated for each tube. Simulation results include local parameters: inlet and outlet qualities, temperatures, enthalpies, entropies, pressure drops, mass flow rate for refrigerant, and inlet and outlet temperatures for air.

Air side heat transfer coefficients are calculated based on the following references : for wavy fins [5], for louvered fins [6]; for slit fins [7].

Refrigerant heat transfer coefficients are calculated: for R-22 and for R-407C evaporation based on [3]; two-phase frictional pressure drop based on [4], void fraction for two-phase acceleration pressure drop based on [8].

2.2 Experimental Calibration Of The Model

Some correlations taken from recent papers can be used without modification but others shall be adapted to the evaporator technology. Heat transfer coefficients have been measured on finned coils on a test rig available at the Center for Energy Studies. A huge number of experimental data have been collected [1, 2]. Finned coils with different numbers of rows, tube diameters, numbers of parallel circuits, numbers of tubes, technologies of fins have been realized and tested for different mass flow rates and air velocities.

The correlations have been tuned to match experimental data with correction factors. These factors, presented in table 1, have been established for all the tested coils.

Table 1 : Correcting factors for the AIR HEX model.

Kim [5]	$0.8 < F_{ext} < 1.0$	Bivens [3] R-22	$1.0 < F_{int} < 1.3$
Wang [6]	without correcting factor	Bivens [3] R-407C	$0.8 < F_{int} < 1.2$
Wang [7]	$1.0 < F_{ext} < 1.05$	Friedel [4]	$0.6 < F_{pl} < 1.35$
F_{int} and F_{pl} depend on fluid and internal diameter (7 or 9.52 mm).			

The deviations between experimental and simulation results are lower than 3 %. Air outlet temperatures are well predicted.

2.3 Experimental/simulation Comparison Of a 3-Row Evaporator

A three-row evaporator prototype has been realized with 7mm diameter tubes and louvered fins (see Figure 1). The three rows of this heat exchanger are physically separated permitting the measurement of intermediate air temperatures. The heat exchanger is composed of three parallel circuits.

For every refrigerant mass flow rate and air velocity the model was run. Figure 2 gives the principal results of the simulation of the three-row evaporator: refrigerant outlet pressure and temperature, air outlet mean temperature.

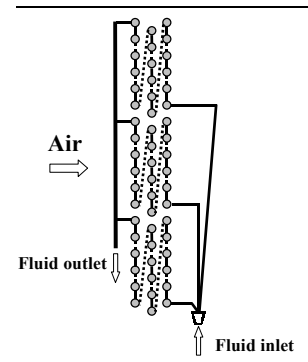


Figure 1 – 3-row heat exchanger lay out.

The maximal difference is $-0.9 / +0.1K$ for the refrigerant outlet temperature and $-0 / +0.5K$ for the air outlet mean temperature. This means that the model can predict the ΔTLM with good precision.

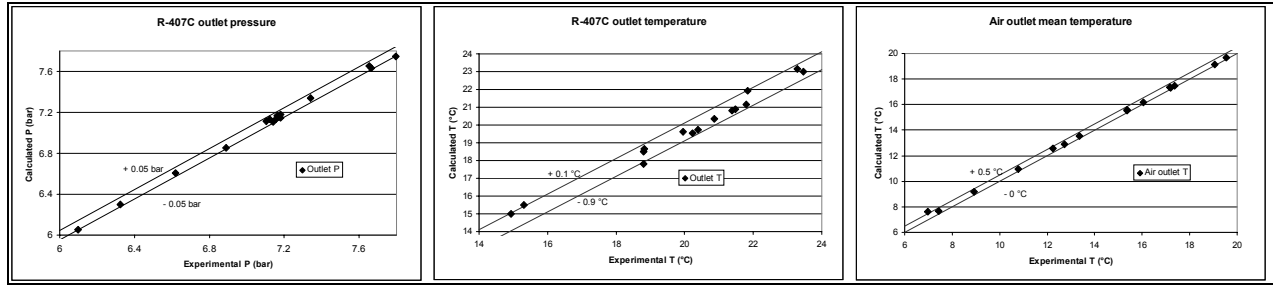


Figure 2 - Principal simulation results of the three-row evaporator.

2.4 Fluid temperature profiles

The model is used to determine the fluid temperature profiles. Since the three circuits are equivalent, only one circuit is studied (Figure 3).

The studied heat exchanger is not a perfect counter-current, and so the refrigerant temperature evolution is not uniform and depends on the current ordinate. The model takes into account an average air temperature for the volume between 2 successive rows.

Figure 4 represents air and refrigerant temperature profiles for the studied circuit of the three-row counter-current evaporator. The x-coordinate axis is divided in 19 points presented in Table 2.

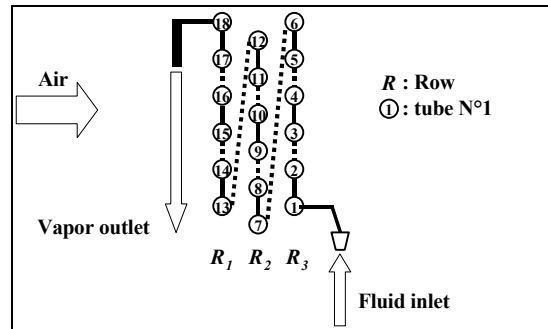


Figure 3 - One circuit of the three-row evaporator.

Table 2 - Calculated temperatures at 19 points of the x-ordinate of curves presented on Figure 4.

Points	Refrigerant R-407C	Air
1	Evapo inlet Temp = $T_{inlet_tube\ N^{\circ}1}$	Mean outlet Temp
2	$T_{outlet_tube\ N^{\circ}1} = T_{inlet_tube\ N^{\circ}2}$	
3 à 6	idem	
7	$T_{outlet_tube\ N^{\circ}6} = T_{inlet_tube\ N^{\circ}7}$	Mean Temp between rows 2 and 3
8 à 12	idem	
13	$T_{outlet_tube\ N^{\circ}12} = T_{inlet_tube\ N^{\circ}13}$	Mean Temp between rows 1 and 2
14 à 18	idem	
19	$T_{outlet_tube\ N^{\circ}18} = \mathbf{Evap\ outlet\ Temp}$	Inlet Temp

For a given refrigerant mass flow rate m_{ref} , if the airflow rate is

- too high the temperature differences (between air and refrigerant) at the evaporator outlet will be the limiting factor (A2, A3, A4, B3, B4, C4).
- too low, the temperature differences (between air and the refrigerant after expansion) will be the limiting factor (B1, C1, C2).

In Figure 4 the optimal air mass flow rates are:

$m_{air} = 180\text{g/s}$ at $m_{ref} = 12\text{g/s}$ (A1), $m_{air} = 260\text{g/s}$ at $m_{ref} = 15\text{g/s}$ (B2) and $m_{air} = 400\text{g/s}$ at $m_{ref} = 20\text{g/s}$ (C3).

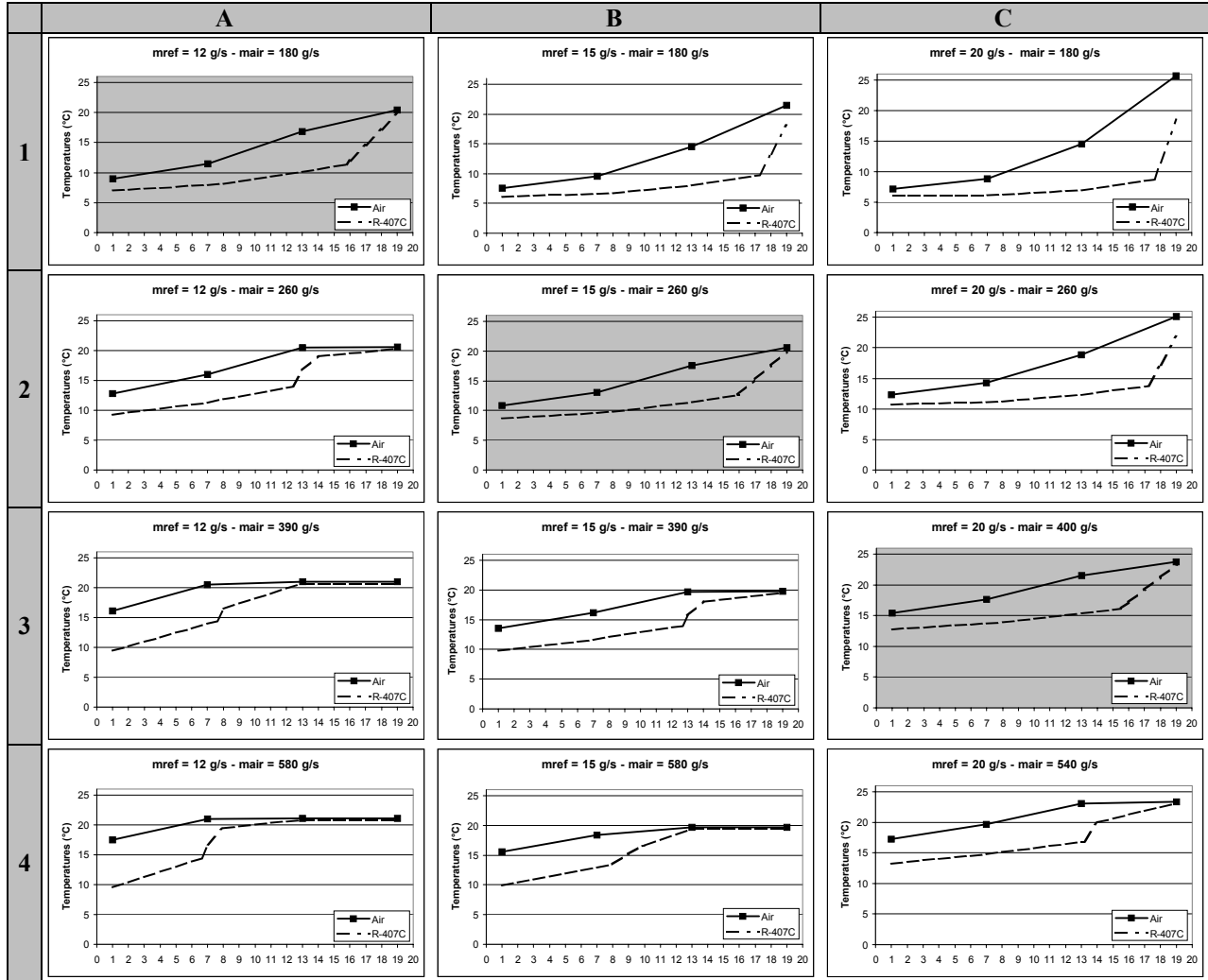


Figure 4 - Temperature evolutions for the three-rows evaporator – See Table 2 for x-ordinate nomenclature.

3. PERFORMANCES OF THE THREE-ROW EVAPORATOR

3.1 Global Heat Exchanger ΔTLM

Figure 5 presents the usual global mean temperature difference ΔTLM variations for the 3 refrigerant mass flow rates and various air mass flow rates. ΔTLM is calculated with R-407C and air inlet and outlet temperatures.

$$\Delta TLM = \frac{(T_{inlet_{air}} - T_{outlet_{ref}}) - (T_{outlet_{air}} - T_{inlet_{ref}})}{\ln \left(\frac{T_{inlet_{air}} - T_{outlet_{ref}}}{T_{outlet_{air}} - T_{inlet_{ref}}} \right)}$$

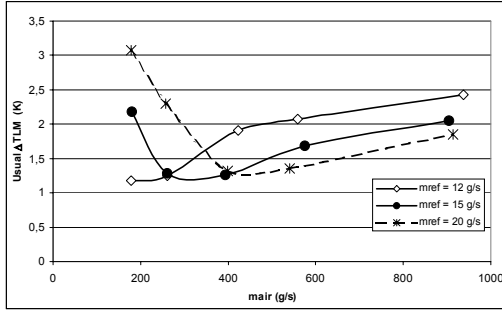


Figure 5 - Usual ΔTLM – 3-row evaporator.

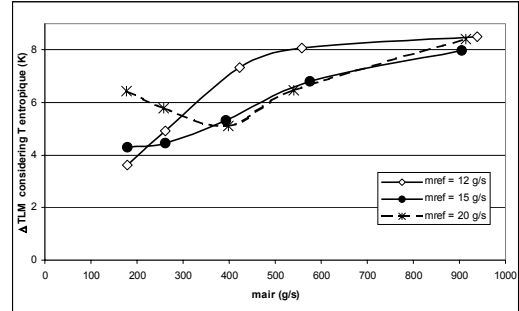


Figure 6 - ΔTLM considering \tilde{T} . 3-row evaporator.

The ΔTLM has also been calculated using the entropic temperature \tilde{T} for R-407C [1].

$$\Delta TLM = \frac{(T_{inlet_{air}} - T_{outlet_{air}})}{\ln\left(\frac{T_{inlet_{air}} - \tilde{T}}{T_{outlet_{air}} - \tilde{T}}\right)}$$

$$\tilde{T} = \frac{h_{outlet_{ref}} - h_{inlet_{ref}}}{s_{outlet_{ref}} - s_{inlet_{ref}}}, \quad \text{where } h : \text{enthalpy}, \quad s : \text{entropy}$$

Results of these calculations are presented Figure 6. Comparison between Figures 5 and 6 underlines how essential the ΔTLM definition is. The two ΔTLM calculations give different results and the optimum air mass flow rates m_{air} cannot be precisely determined.

The ΔTLM approach for counter-current or co-current flow arrangements is adapted when the temperature difference ΔT varies linearly with the heat flow rate over the whole exchanger. Evaporation and superheat imply huge variation of heat capacities, and the mean effective temperature difference does not make sense. Consequently, the conductance UA calculated using global ΔTLM is wrong, and does not permit to define optimum design of the heat exchanger.

3.2 ΔTLM calculated based on enthalpy zones

Using AIR_HEX the beginning of superheat can be precisely defined. So 2 ΔTLM s can be calculated for evaporation and superheat zones. Based on the respective length of the two zones, a global average ΔTLM can be calculated. Figure 7 presents the relative variations of this average ΔTLM . Nevertheless these average ΔTLM cannot be used to determine the optimum performance of the evaporator.

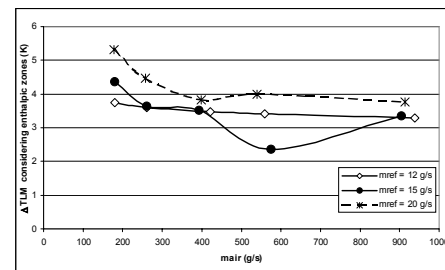


Figure 7 - ΔTLM based on the enthalpy zones.

Comparing Figure 7 and Figure 4, it is obvious that the optimum mass flow rates based on these mean ΔTLM s correspond to higher air mass flow rates where the last row is useless and do not correspond to the optimal design.

3.3 Row Average ΔTLM

Calculation of a global ΔTLM averaging the 3-row ΔTLM has been performed. Results are presented Figure 8.

Analyzing Figure 8 and Figure 4, results indicate that this average value of ΔTLM does not permit either to define optimum design.

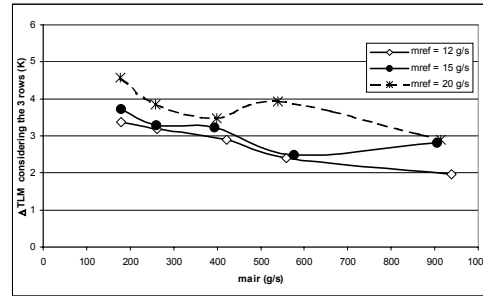


Figure 8 - ΔTLM considering the 3 rows.

3.4 Tube-by-tube Average ΔTLM

Figure 4 indicates that the optimum configuration corresponds to parallel temperature profile between refrigerant and air. The thermal irreversibilities are minimum when the difference between the two fluid temperatures is also minimum. So, the ideal operation of the heat exchanger is determined by similar or parallel temperature profiles with a difference as small as possible.

AIR_HEX permits to calculate the temperature difference at each point of the heat exchanger. The ΔTLM of each tube is calculated. ΔTLM^* represents the average of the 18 ΔTLM s calculated for each tube. The smaller this ΔTLM^* , the closer the temperature evolutions of refrigerant and air.

The average_deviation* is the measure of the value dispersion referred to the mean value. The smaller the ΔTLM average_deviation*, the closer the gradient between the two fluids.

Then, the smaller the product ($\Delta TLM^* \times$ average_deviation*) or the larger $\Psi^* = 1 / (\Delta TLM^* \times$ average_deviation*), the more parallel the temperature profiles with a small difference.

The best operating conditions of a heat exchanger correspond to the maximum of the Ψ^* parameter.

$$\Psi^* = \frac{1}{\Delta TLM^* \times \text{average_deviation}^*} \quad \text{with } \text{average_deviation}^* = \sqrt{\frac{n \sum \Delta TLM^2 - (\sum \Delta TLM)^2}{n(n-1)}}$$

Figure 9 and 10 present respectively the average_deviation* and the Ψ^* parameter for the different measured points.

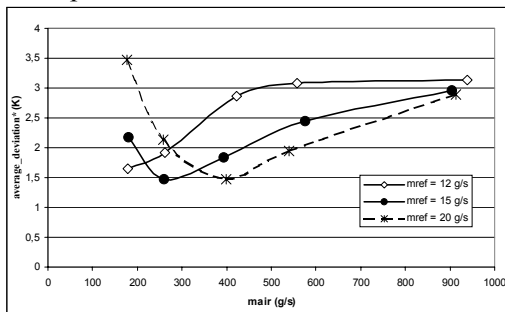


Figure 9 - average_deviation*.

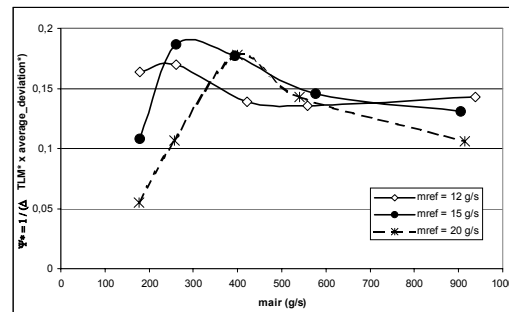


Figure 10 - $\Psi^* = 1/(\Delta TLM^* \times$ average_deviation*) of the three-row evaporator.

Figure 10 permits to determine precisely the optimum air mass flow rates. For $m_{ref} = 12\text{g/s}$, the optimum air mass flow rate is $m_{air} = 230\text{g/s}$, for $m_{ref} = 15\text{g/s}$, $m_{air} = 300\text{g/s}$, and for $m_{ref} = 20\text{g/s}$, $m_{air} = 400\text{g/s}$. These air mass flow rates match with those which can be determined from figure 4 (A1, B2, C3).

4. USE OF THE ψ^* CRITERION FOR SETTING THE NUMBER OF ROWS

The ψ^* criterion is used to determine the optimum number of rows for a counter-current evaporator. The 18 tubes of each circuit are set to compose counter-current evaporator with $N_r = 2, 3, 4$ or 5 rows (see figure 11).

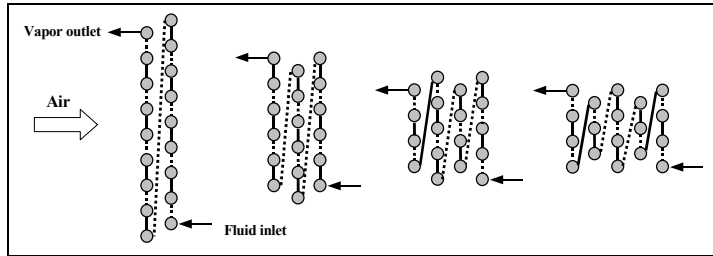


Figure 11 - Configuration of one circuit.

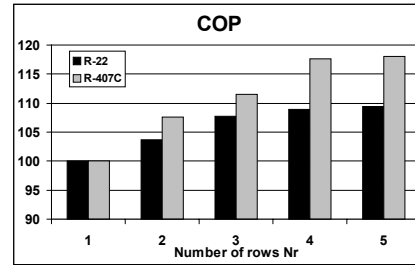


Figure 12 - COP for the three-row evaporator.

A software called SPLIT-DESIGN [2] has been developed to calculate refrigerating cycle of AC system. It permits to calculate the COP of a given system. It has been used to analyze the impact of the number of rows of the evaporator while condenser surface and mass flow rates (air and refrigerant) have been kept constant.

Figure 12 presents the COP of multi-row evaporator compared to the single-row one, both for R-22 and R-407C. For each refrigerant, the COP increases with the number of rows because the frontal section area decreases, so the air velocity increases (from 0.33 to 1.67m/s) and the external heat transfer coefficient increases. It can be noticed that the COP improvement of R-407C is significantly higher compared to R-22.

For both fluids, Figures 13 and 14 present the ΔTLM^* , the average_deviation* and the Ψ^* parameter. Figure 13 indicates that the 2 average ΔTLM^* are nearly equal whatever the number of rows.

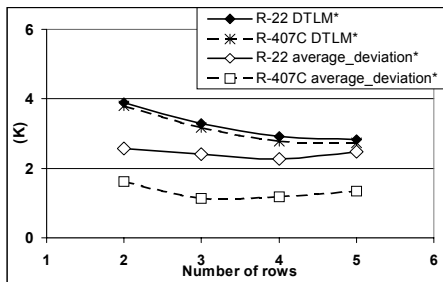


Figure 13 - ΔTLM^* , average_deviation* R-22 and R-407C

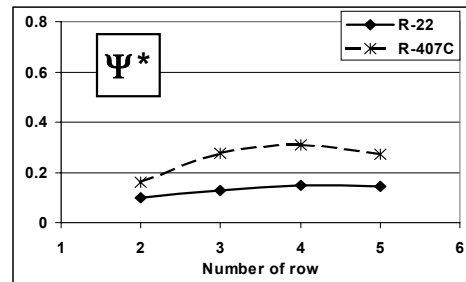


Figure 14 - Ψ^* R-22 and R-407C.

The average_deviation* are half less for R-407C, which means that profiles between R-407C and air are more parallel compared to R-22 yielding to a better COP. For R-407C, the Ψ^* permits to determine the optimum number of rows (4) for an air mass flow rate $m_{air} = 270\text{g/s}$ (figure 14).

5. CONCLUSIONS

The determination of the usual global ΔTLM and the corresponding UA cannot be used to determine the optimum mass flow rates (air and refrigerant) for heat exchanger design.

The calculation of an average ΔTLM based on evaporation and superheat zones permits only to verify that the global heat transfer coefficient of the heat exchanger is higher at high air velocities.

A tube by tube average ΔTLM calculation permits to determine a Ψ^* factor used to calculate optimum refrigerant mass flow rate corresponding to a given airflow rate of multiple-row heat exchanger. The method requires a tube-by-tube calculation permitting to lower the temperature differences between airflow and a zeotropic mixture as R-407C.

REFERENCES

- [1] Bigot G., Palandre L. and Clodic D., "Optimized design of heat exchangers for "reversible" heat pump using R-407C", Proc. 2000 Int'l Refrigeration Conference, Purdue University, West Lafayette, Ind. USA, pp. 39-46.
- [2] Bigot G., "Etude et conception de systèmes air/air inversables utilisant des mélanges à glissement de température," Ph D. thesis, Ecole des Mines de Paris, Center for Energy Studies, 2001.
- [3] Bivens JD.B and Yokozeki A., "Heat transfer coefficients and transport properties for alternative refrigerants", Proc. 1994 International Refrigeration Conference, Purdue University, West Lafayette, Ind. USA, p 299-303.
- [4] Friedel L., "Improved friction pressure drop calculations for horizontal and vertical two-phase pipe flow", European Two-Phase flow group meeting, Ispra, Italy, Paper E2.
- [5] Kim N.H., Youn B. and Webb R.L., "Air side heat transfer and friction correlations for plain fin-and-tube heat exchangers with staggered tube arrangement", J. Heat Transfer, Vol. 121, p 662-667.
- [6] Wang C.C., LEE C.J., Chang C.T. and Lin S.P., "Heat transfer and friction correlation for compact louvered fin-and-tube heat exchangers", Int. J of Heat and Mass Transfer, Vol. 42, p 1945-1956.
- [7] Wang C.C., Tao W.H. and Chang C.J., "An investigation of the slit fin-and-tube heat exchangers", Int. J of Refrigeration, Vol. 22, p 595-603.
- [8] Zivi S.M., "Estimation of steady-state steam void-fraction by means of the principle of minimum entropy production", J. of Heat Transfer, Vol. 86c, p 247-252.